Supporting Information

(*M*)- and (*P*)-bicelaphanol A, Dimeric Trinorditerpenes with Promising Neuroprotective Activity from *Celastrus orbiculatus*

Luo-Yi Wang,† Jian Wu,† Zhuo Yang,† Xu-Jie Wang, Yan Fu, Shuang-Zhu Liu, Hong-Min Wang, Wei-Liang Zhu, Hai-Yan Zhang* and Wei-Min Zhao*

State Key Laboratory of Drug Research, Shanghai Institute of Materia Medica, Chinese Academy of Sciences, Shanghai 201203, People's Republic of China

† *These authors contributed equally to this work.*

* *To whom correspondence should be addressed. E-mail: hzhang@mail.shcnc.ac.cn (H. Y. Zhang); wmzhao@mail.shcnc.ac.cn (W. M. Zhao), Tel & Fax: +86-21-50806052.*

Contents

1. LC-MS/MS Spectra of (*M*)-bicelaphanol A (1), (*P*)-bicelaphanol A (2) and the Crude Extract of *Celastrus orbiculatus*

In order to know if compounds **1** and **2** are biotic material or artifacts formed during the isolation procedures, liquid chromatography-tandem mass spectrometry (LC-MS/MS) was employed to qualitatively determine **1** and **2** in the crude extract of *Celastrus orbiculatus.*

Appropriate amounts of compounds **1**, **2** and root bark of *C. orbiculatus* were dissolved in 95% EtOH and kept at room temperature for about 2 hours. The resulting solutions were syringe-filtered through a 0.45 μm nylon filter to make the standard solutions of **1**, **2** and the crude extract sample, respectively. LC-MS/MS analysis was performed using a Finnigan LCQ Deca system equipped with a Cnwsil C_{18} column (2.1 mm × 100 mm, 3.5 μm). The mobile phase consisted of water with 0.2‰ HCOOH (A phase) and acetonitrile (B phase). Gradient: 60-100% B in 25 min. Tests were carried out at 40 °C with a flow rate of 0.3 mL/min. The $[M-H]^-$ ion at *m/z* 557 of the standard solutions of **1**, **2** and the crude extract sample was measured using the selective ion monitoring mode.

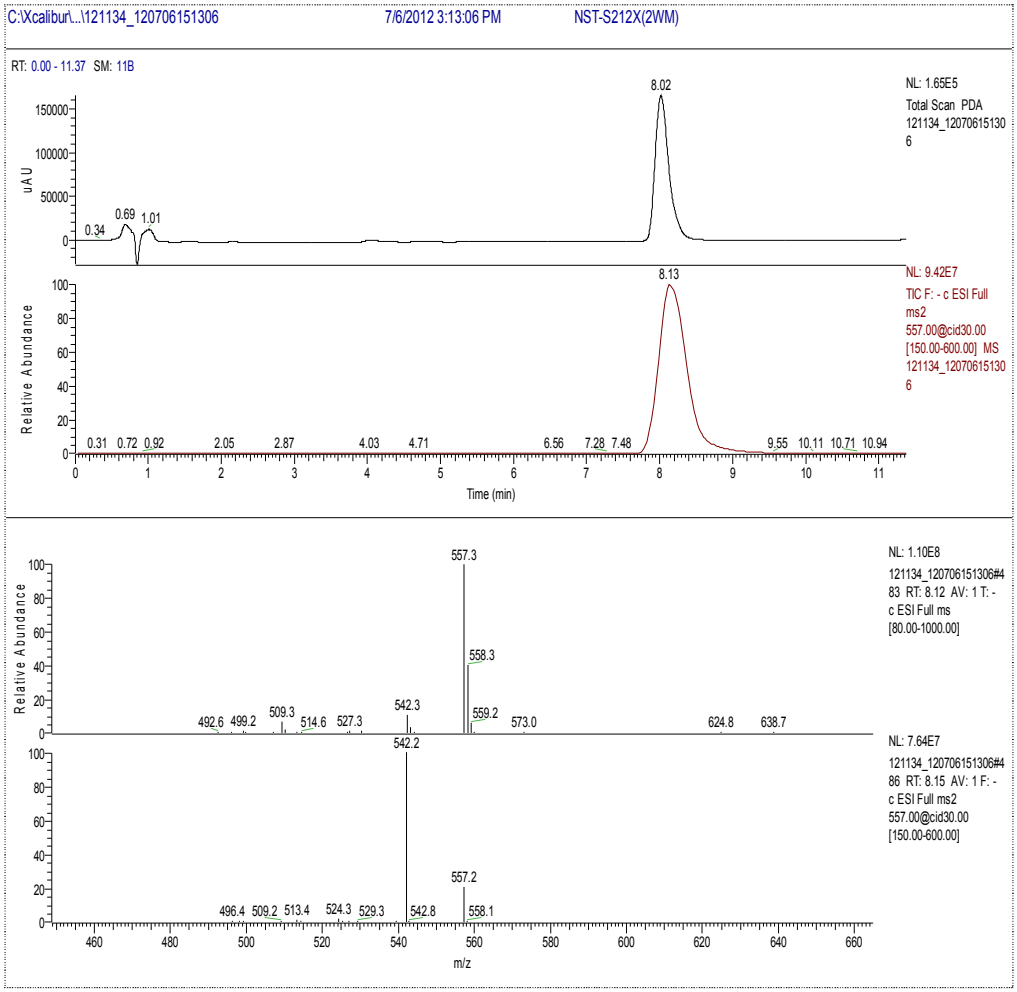

Figure S1. LC-MS/MS spectrum of $[M-H]^-$ at *m/z* 557 of (*M*)-bicelaphanol A (**1**).

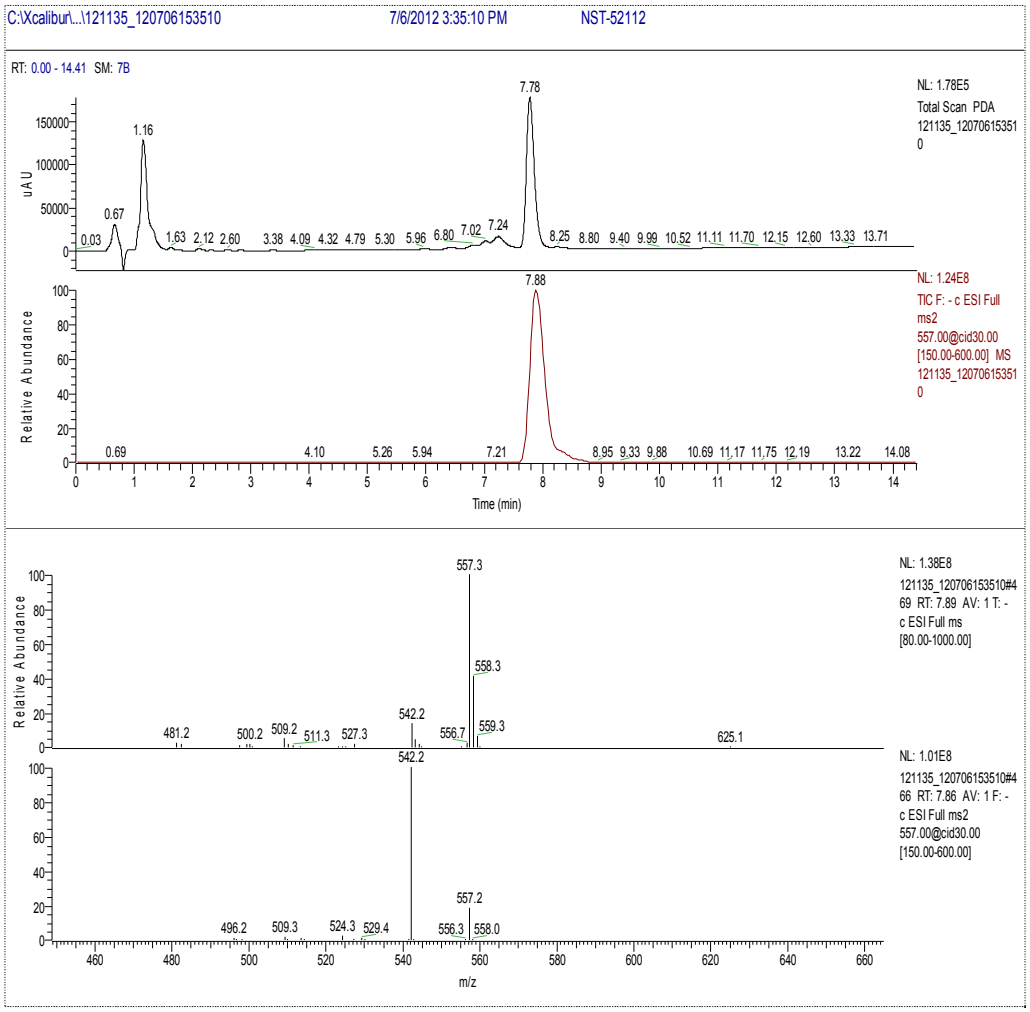

Figure S2. LC-MS/MS spectrum of $[M-H]^-$ at *m/z* 557 of (*P*)-bicelaphanol A (**2**).

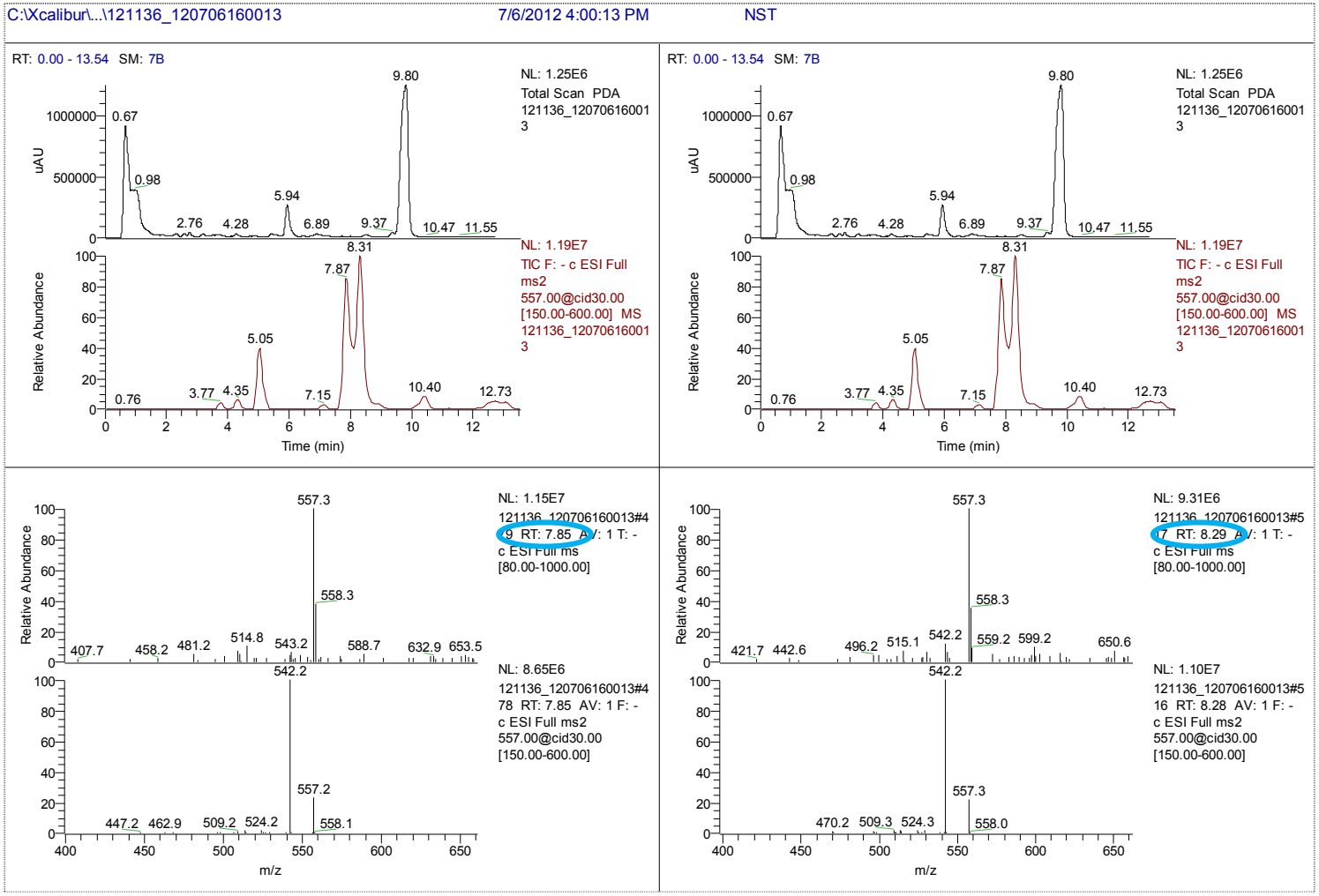

Figure S3. LC-MS/MS spectrum of $[M-H]^-$ at *m/z* 557 of the crude extract sample.

As shown in Figure S1-S3, the *m/z* 557 ions of the crude extract sample gave MS/MS spectra of the same fragmentation pattern at very similar retention time as those of compounds **1** and **2**, indicating the presence of **1** and **2** in the crude extract. Thus, compounds **1** and **2** were confirmed to be naturally occurring products rather than artifacts formed during isolation and purification. A plausible biogenetic pathway for (*M*)-bicelaphanol A (**1**) and (*P*)-bicelaphanol A (**2**) was proposed as shown in Scheme S1.

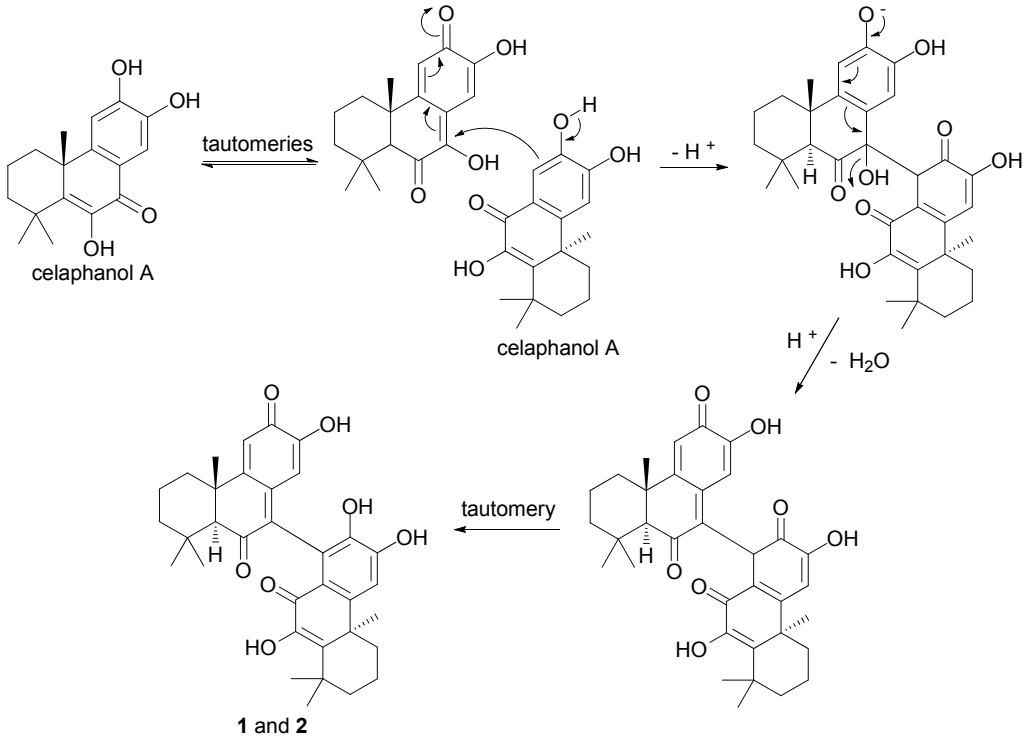

Scheme S1. Plausible biosynthetic pathway of **1** and **2**.

2. Characterization Data of Celaphanol A (3)

Celaphanol A (**3**): red amorphous powder; $[\alpha]^{22}_{D}$ -34.1 (*c* 0.9, $CDCl_3$), $[\alpha]^{20}_{D}$ 20.9 (*c* 0.9, acetone), $[\alpha]^{20}_{D}$ 22.8 (*c* 0.9, MeOH); ECD (MeOH): 210 nm (Δε +32.9), 223 nm (Δε -8.5), 280 nm (Δε +47.5), 321 nm (Δε -34.8); ^{1}H NMR (pyridine-d_5, 400 MHz), ^{13}C NMR (pyridine-d_5, 100 MHz), ^{1}H NMR (acetone-d_6, 400 MHz) and ^{13}C NMR (acetone-d_6, 100 MHz) data, see Table S1; ESI (positive) *m/z* 289 $[M+H]^+$; ESI (negative) *m/z* 287 $[M-H]^-$, 575 $[2M-H]^-$; HRESIMS m/z 575.2635 $[2M-H]^-$ (calcd for $C_{34}H_{39}O_8$, 575.2645). The solvent 'CDCl$_3$' reported for the optical rotation of celaphanol A in the literature (*Phytochemistry*, 1999, 51, 683-687) has been confirmed by Dr. Hongquan Duan, one of the authors of the paper, to be a typo. The absolute configuration at C-10 of **3** was deduced to be *R* by comparison of its experimental ECD spectrum with the calculated ECD spectrum (Figure 4 and Figure 5).

Table S1. ^{1}H and ^{13}C NMR data for celaphanol A (**3**) in pyridine-d_5 and acetone-d_6

	3[a]		**3**[b]	
no.	δ_H	δ_C	δ_H	δ_C
1	2.32/1.77, m	33.9, CH_2	2.39/1.77, m	34.1, CH_2
2	1.78/1.63, m	17.9, CH_2	1.92/1.72, m	18.1, CH_2
3	1.90/1.38, m	38.1, CH_2	1.98/1.45, m	38.4, CH_2
4		36.1, C		36.4, C
5		140.2, C		140.6, C
6		145.2, C	-OH, 7.48, s	144.6, C
7		180.1, C		179.9, C
8		121.0, C		121.1, C
9		149.4, C		150.0, C
10		40.4, C		40.8, C
11	7.42, s	113.1, CH	7.06, s	112.7, CH
12		153.6, C		151.9, C
13		146.4, C		144.9, C
14	8.24, s	112.4, CH	7.50, s	112.1, CH
15	1.53, s	27.9, CH_3	1.41, s	27.9, CH_3
16	1.56, s	28.4, CH_3	1.43, s	28.4, CH_3
17	1.62, s	35.4, CH_3	1.50, s	35.2, CH_3

[a] Data were recorded in pyridine-d_5; [b] data were recorded in acetone-d_6.

3. Optimized Structures and Calculated Energies of 1 and 2

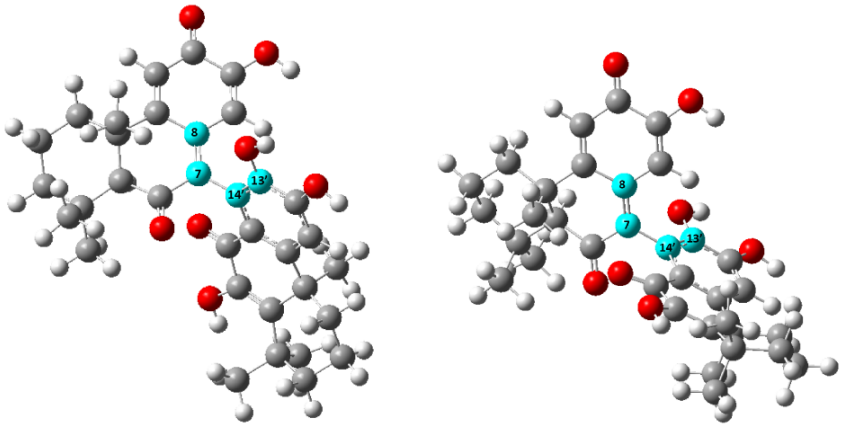

Figure S4. Optimized structures of (*M*)-bicelaphanol A (**1**) and (*P*)-bicelaphanol A (**2**). Left: (*M*)-bicelaphanol A (**1**), the C8-C7-C14'-C13' torsion angle is 69.58°; right: (*P*)-bicelaphanol A (**2**), the C8-C7-C14'-C13' torsion angle is -84.02°. It is pointed out that the C8-C7-C14'-C13' torsion angle in the optimized structures of **1** is closely similar to that found experimentally by X-ray crystallography (66.38°).

Table S2. Energy scan at the B3LYP/6-31G(d,p) level

dihedral angle	E(au)	ΔE(au)	ΔE(kcal/mol)	ΔE(kJ/mol)
-100.0000	-1845.08550900	-0.05076720	-31.85692567	-132.8433801
-90.0000	-1845.08611720	-0.05137540	-32.23857725	-134.4348671
-84.0185	**-1845.08610070**	**-0.05135890**	**-32.22822334**	**-134.3916913**
-80.0000	-1845.08605100	-0.05130920	-32.19703609	-134.2616405
-70.0000	-1845.08559340	-0.05085160	-31.90988752	-133.0642309
-60.0000	-1845.08366770	-0.04892590	-30.70149151	-128.0252196
-50.0000	-1845.04278210	-0.00804030	-5.045368653	-21.03918728
-40.0000	-1845.04429990	-0.00955810	-5.997803331	-25.01083989
-30.0000	-1845.04409630	-0.00935450	-5.870042295	-24.47807637
-20.0000	-1845.03474180	0.00000000	0	0
-10.0000	-1845.04515850	-0.01041670	-6.536583417	-27.25755285
0.0000	-1845.05503740	-0.02029560	-12.73569196	-53.10783546
10.0000	-1845.06389770	-0.02915590	-18.29561881	-76.29273043
20.0000	-1845.07141510	-0.03667330	-23.01286248	-95.96363655
30.0000	-1845.07749970	-0.04275790	-26.83100983	-111.885311
40.0000	-1845.08217250	-0.04743070	-29.76323856	-124.1127048
50.0000	-1845.08527470	-0.05053290	-31.70990008	-132.2302833
60.0000	-1845.08694820	-0.05220640	-32.76003806	-136.6093587
69.5787	**-1845.08750250**	**-0.05276070**	**-33.10786686**	**-138.0598048**
70.0000	-1845.08750200	-0.05276020	-33.1075531	-138.0584964
80.0000	-1845.08700080	-0.05225900	-32.79304509	-136.746998
90.0000	-1845.08599080	-0.05124900	-32.15925999	-134.1041142
100.0000	-1845.08436970	-0.04962790	-31.14200353	-129.8621547

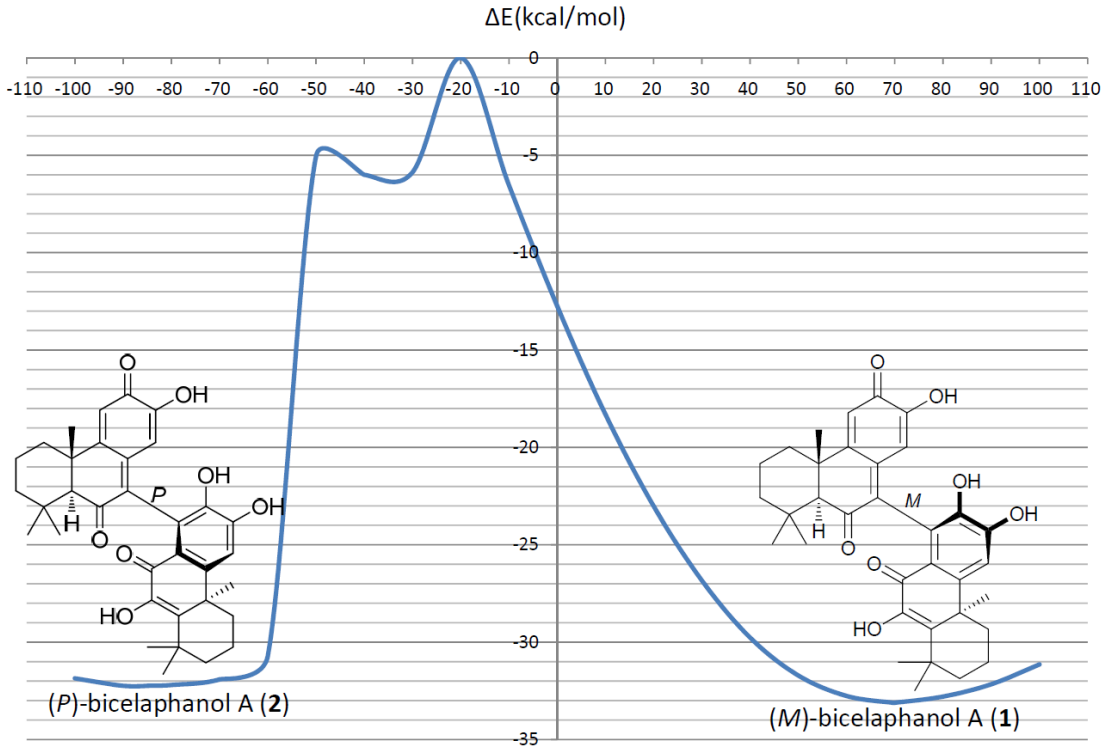

Figure S5. Energy scan at the B3LYP/6-31G(d,p) level. The C8-C7-C14'-C13' dihedral angle changes from -100° to +100°.

4. NMR, HRESIMS and IR Spectra of Compounds 1-3

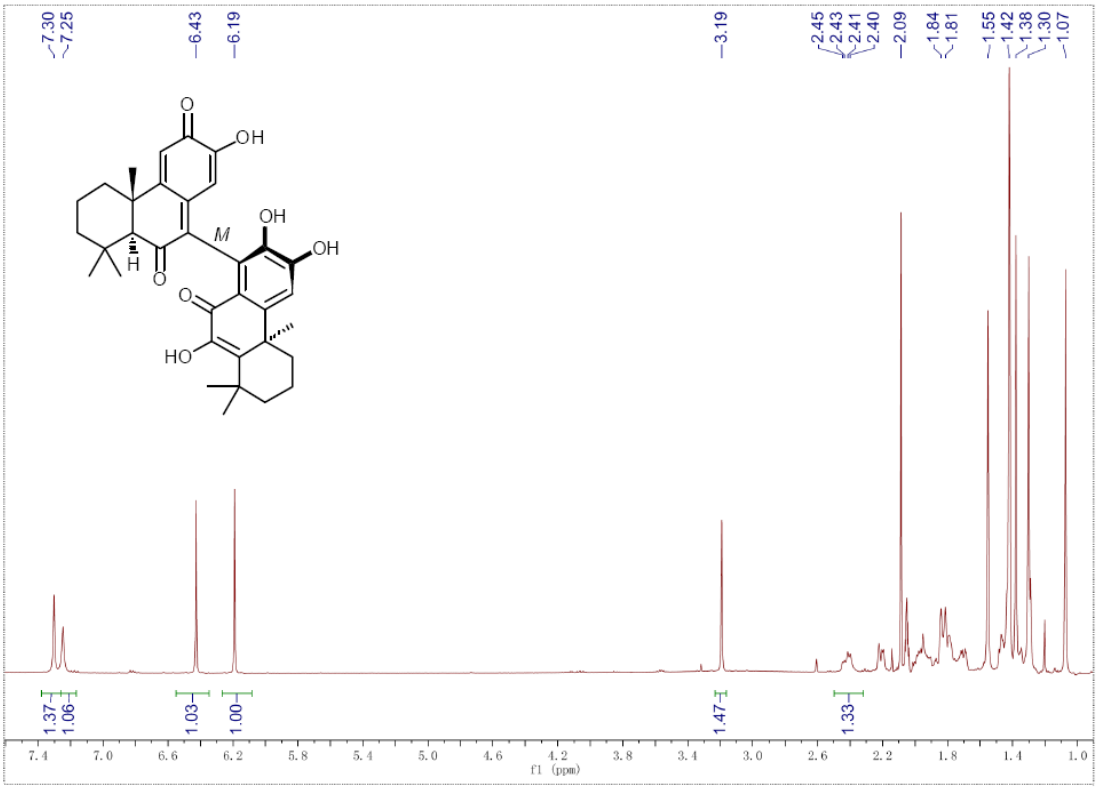

Figure S6. ^{1}H NMR spectrum of (*M*)-bicelaphanol A (**1**) in acetone-d_6 (400 MHz).

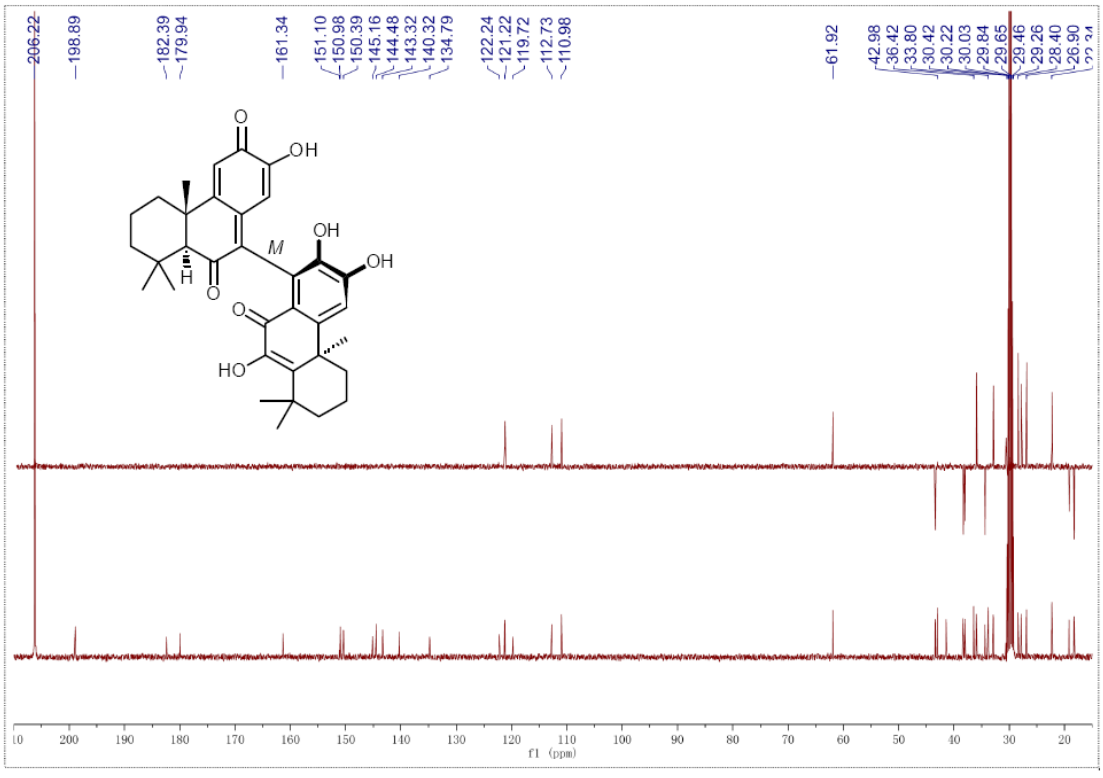

Figure S7. ^{13}C NMR spectrum of (*M*)-bicelaphanol A (**1**) in acetone-d_6 (100 MHz).

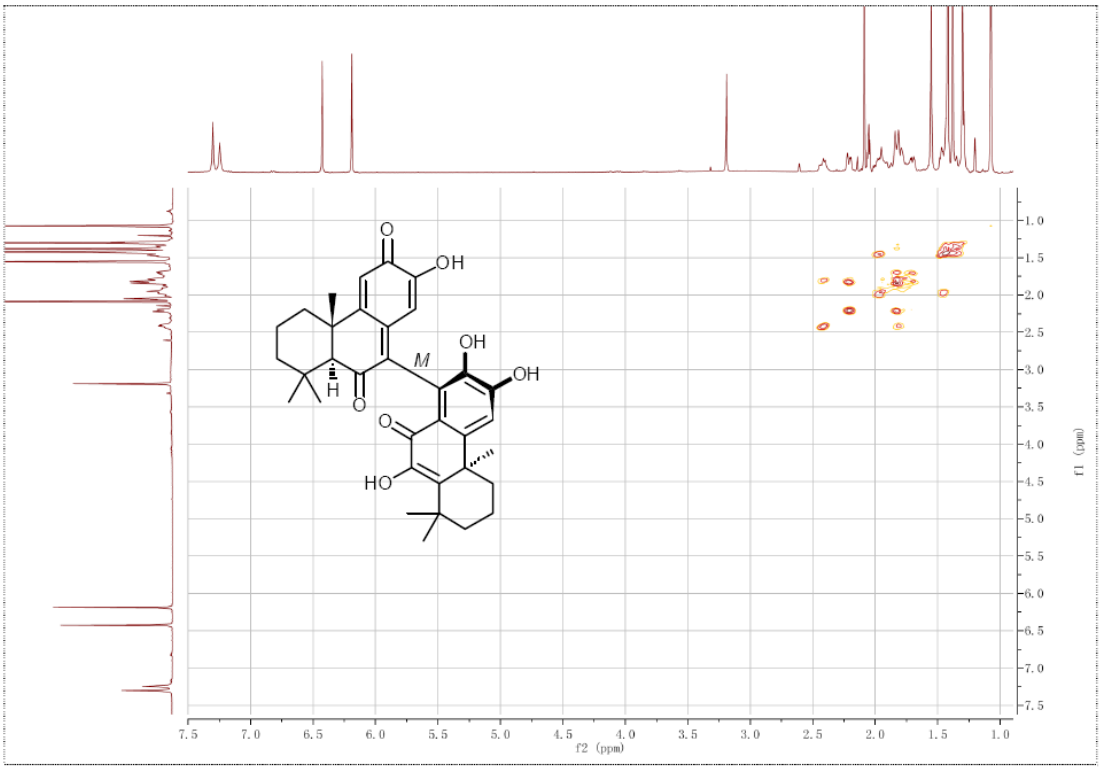

Figure S8. ^{1}H-^{1}H COSY spectrum of (*M*)-bicelaphanol A (**1**) in acetone-d_6.

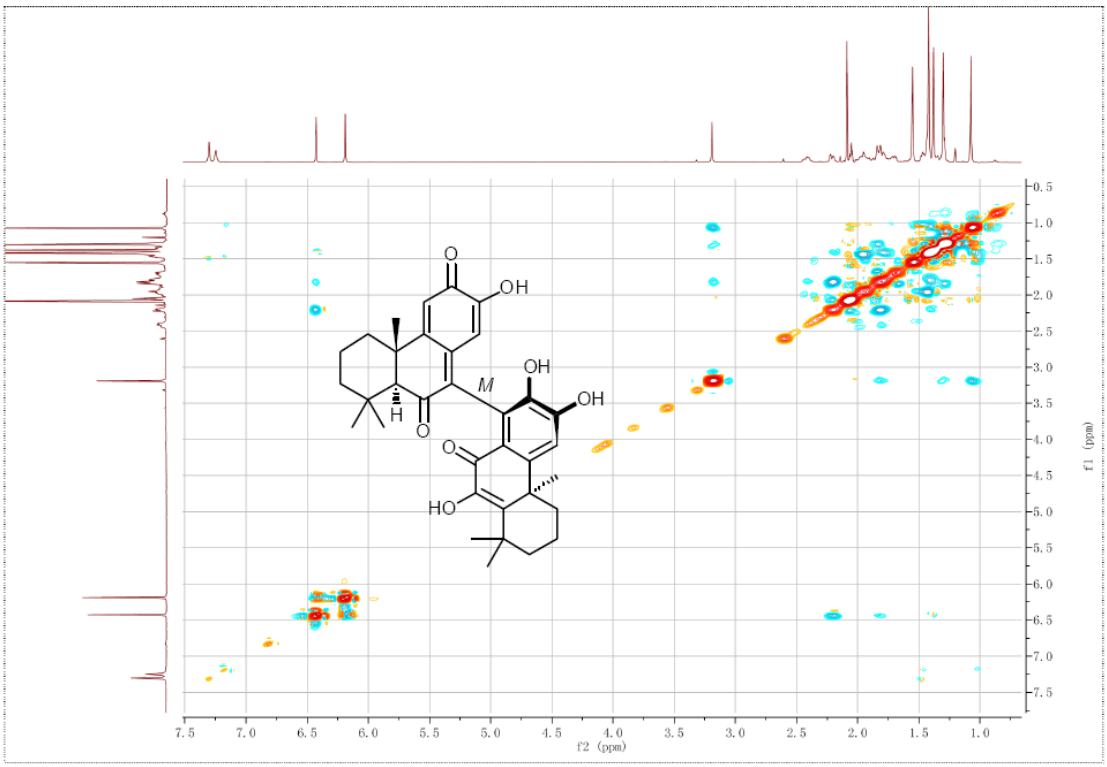

Figure S9. NOESY spectrum of (*M*)-bicelaphanol A (**1**) in acetone-d_6.

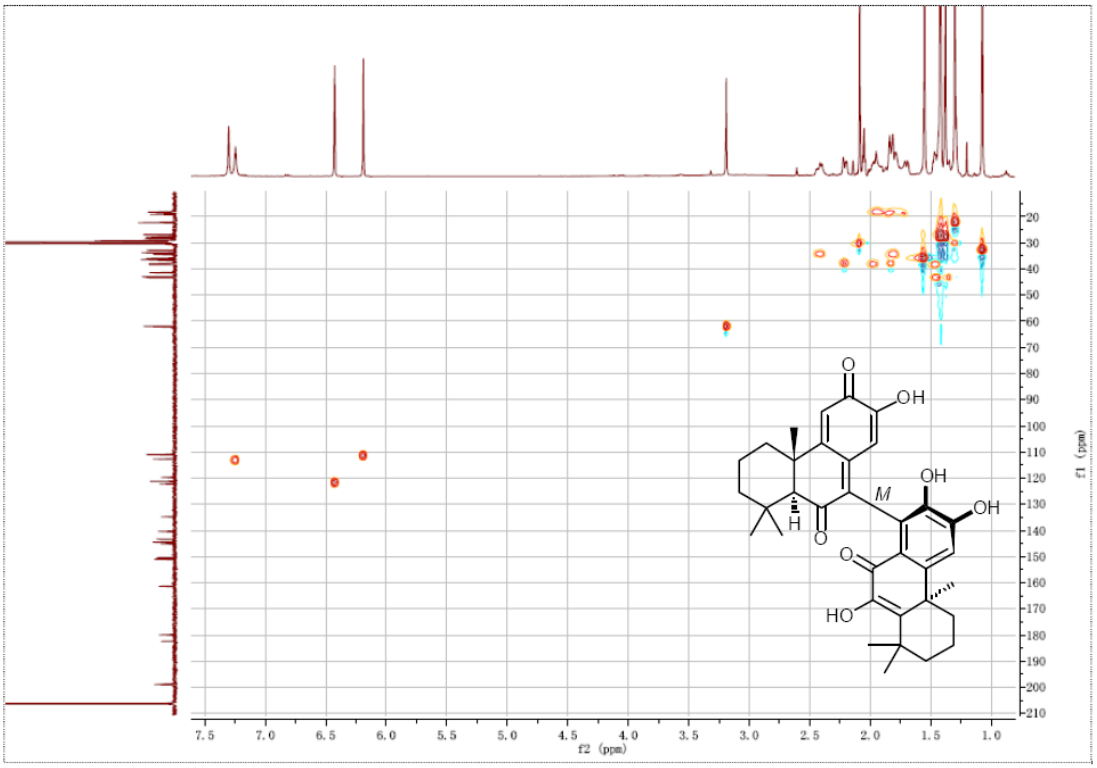

Figure S10. HSQC spectrum of (*M*)-bicelaphanol A (**1**) in acetone-d_6.

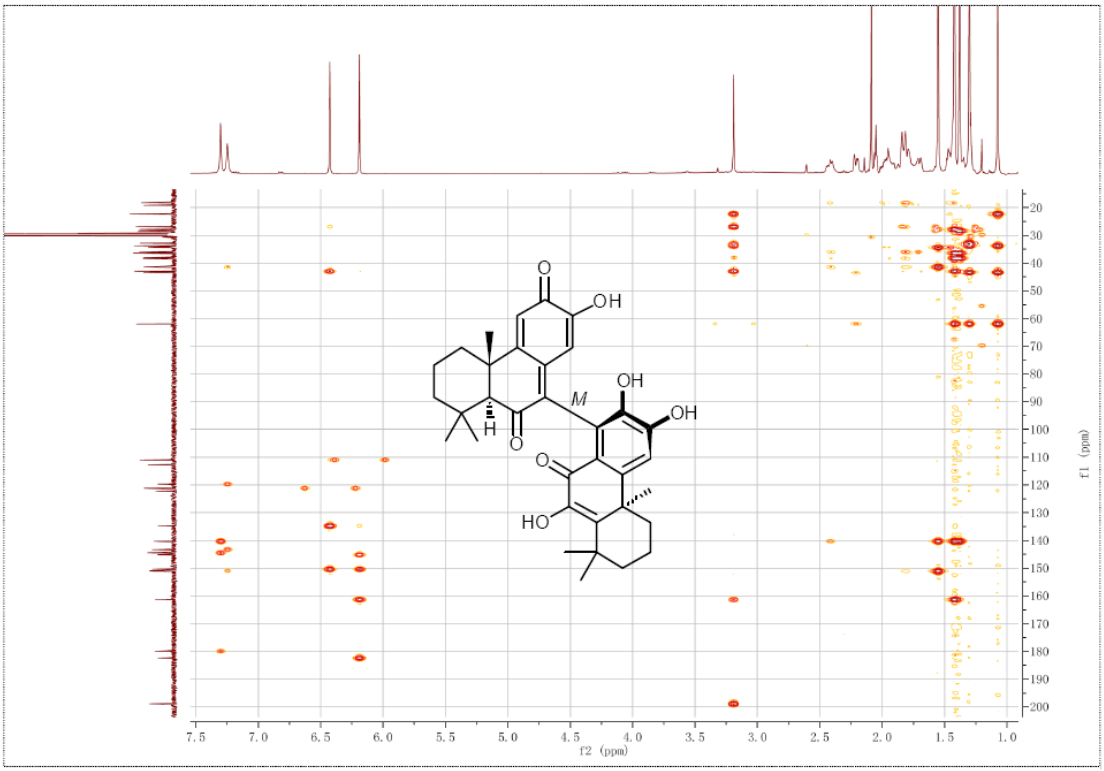

Figure S11. HMBC spectrum of (*M*)-bicelaphanol A (**1**) in acetone-d_6.

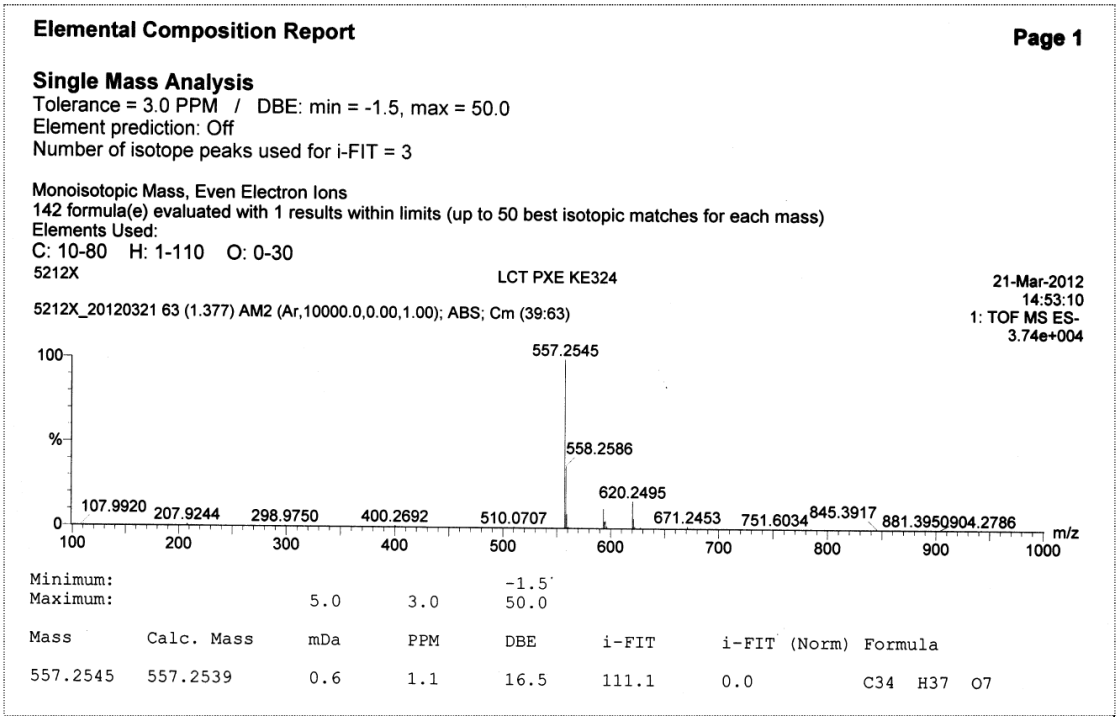

Figure S12. HRESIMS spectrum of (*M*)-bicelaphanol A (**1**).

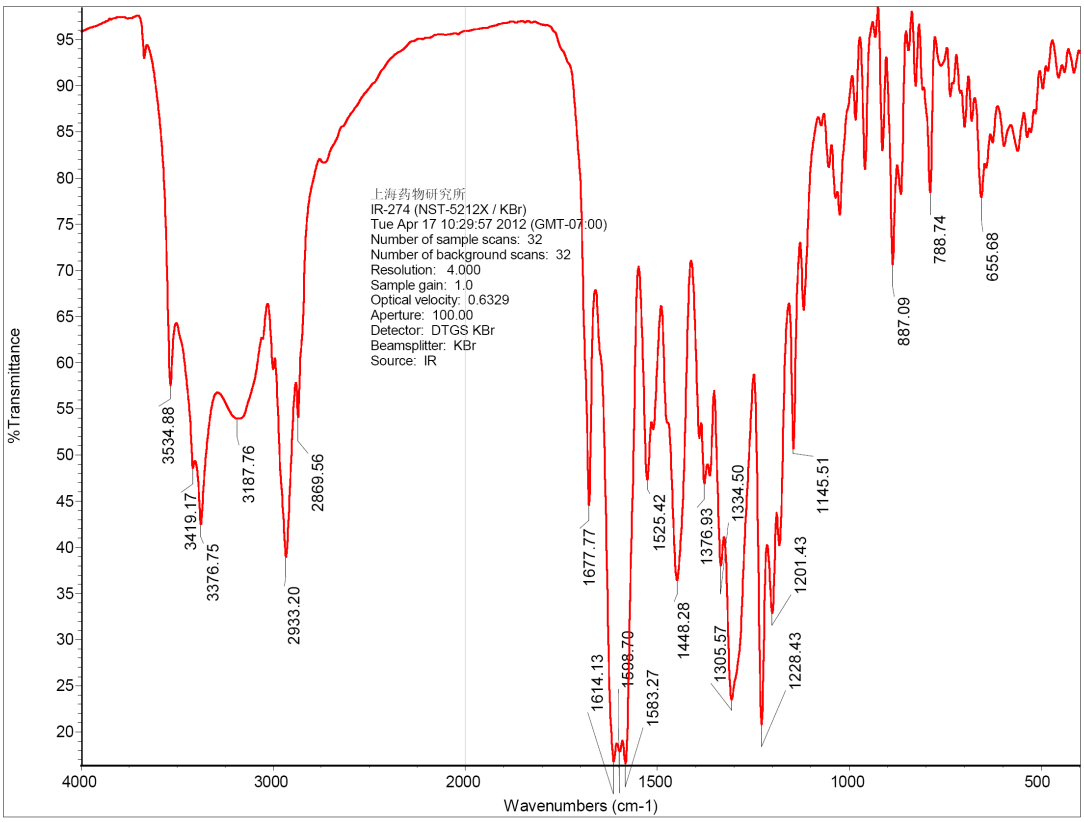

Figure S13. IR spectrum of (*M*)-bicelaphanol A (**1**).

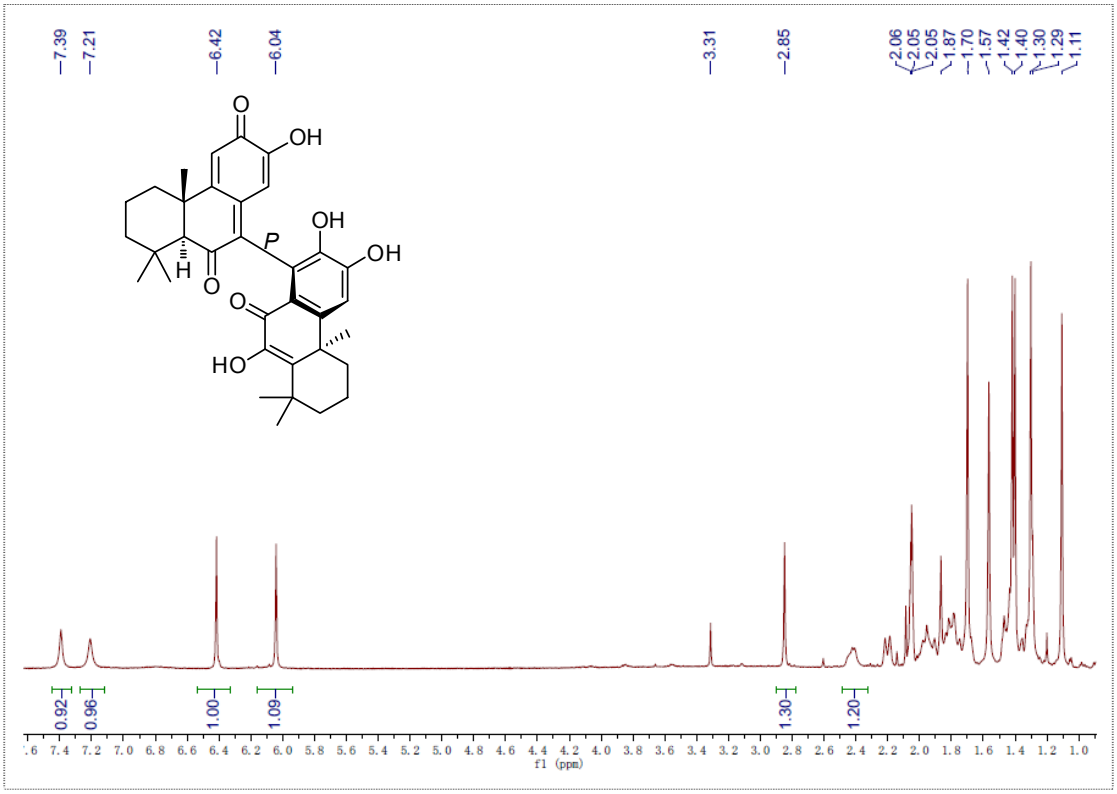

Figure S14. [1]H NMR spectrum of (*P*)-bicelaphanol A (**2**) in acetone-d_6 (400 MHz).

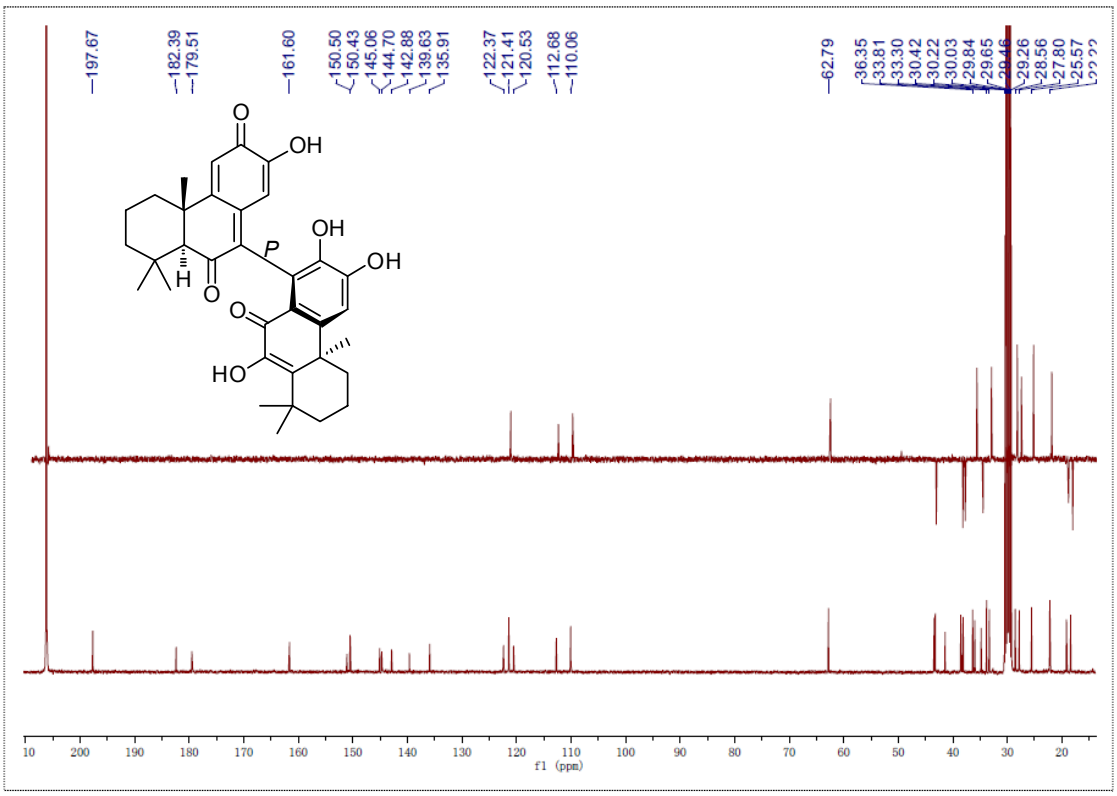

Figure S15. [13]C NMR spectrum of (*P*)-bicelaphanol A (**2**) in acetone-d_6 (100 MHz).

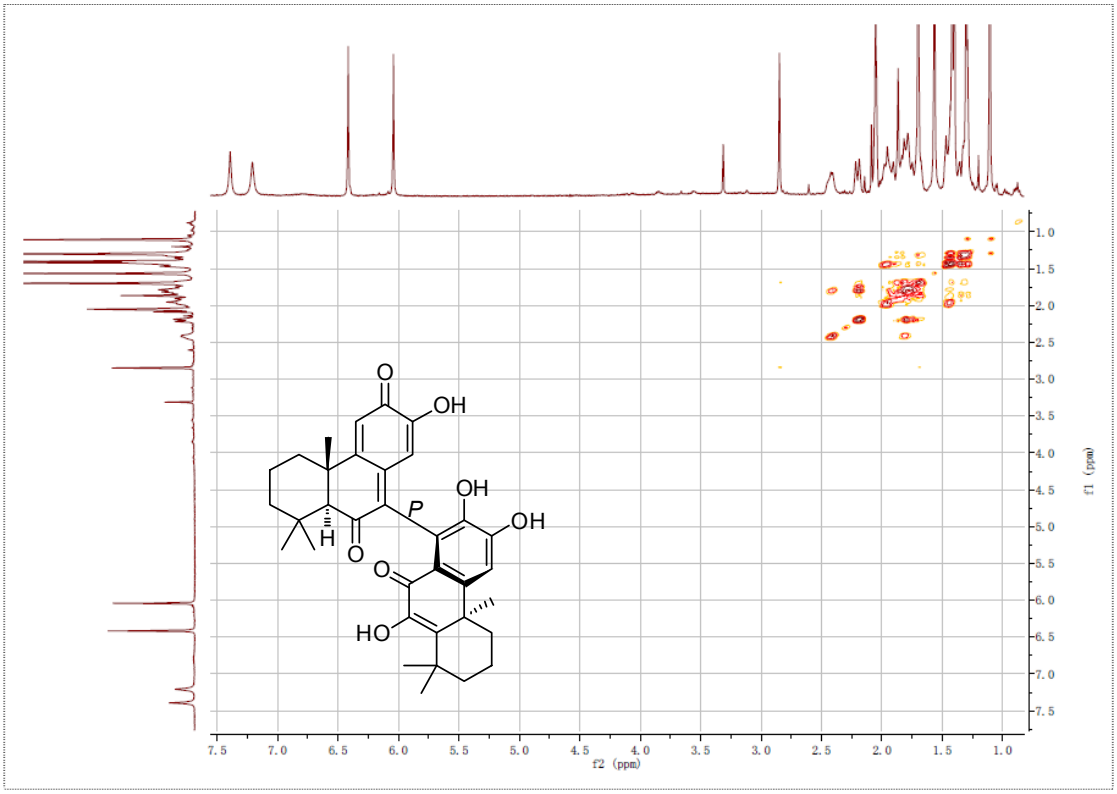

Figure S16. ^{1}H-^{1}H COSY spectrum of (*P*)-bicelaphanol A (**2**) in acetone-d_6.

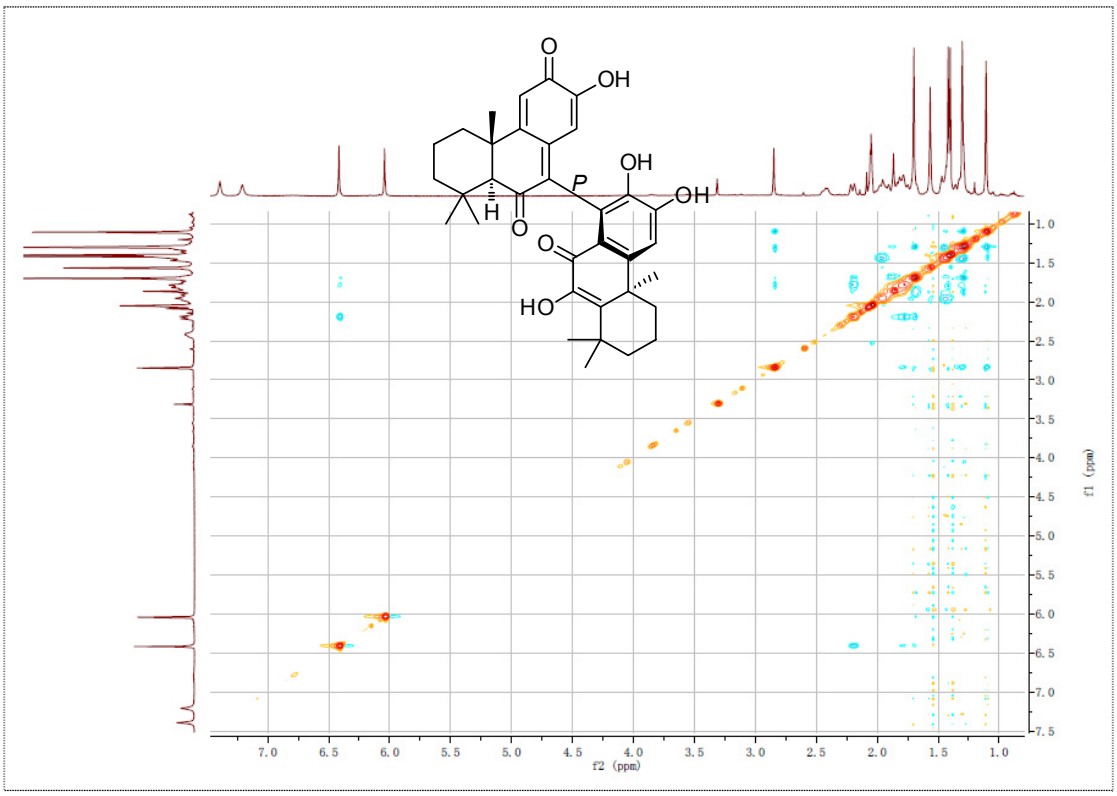

Figure S17. NOESY spectrum of (*P*)-bicelaphanol A (**2**) in acetone-d_6.

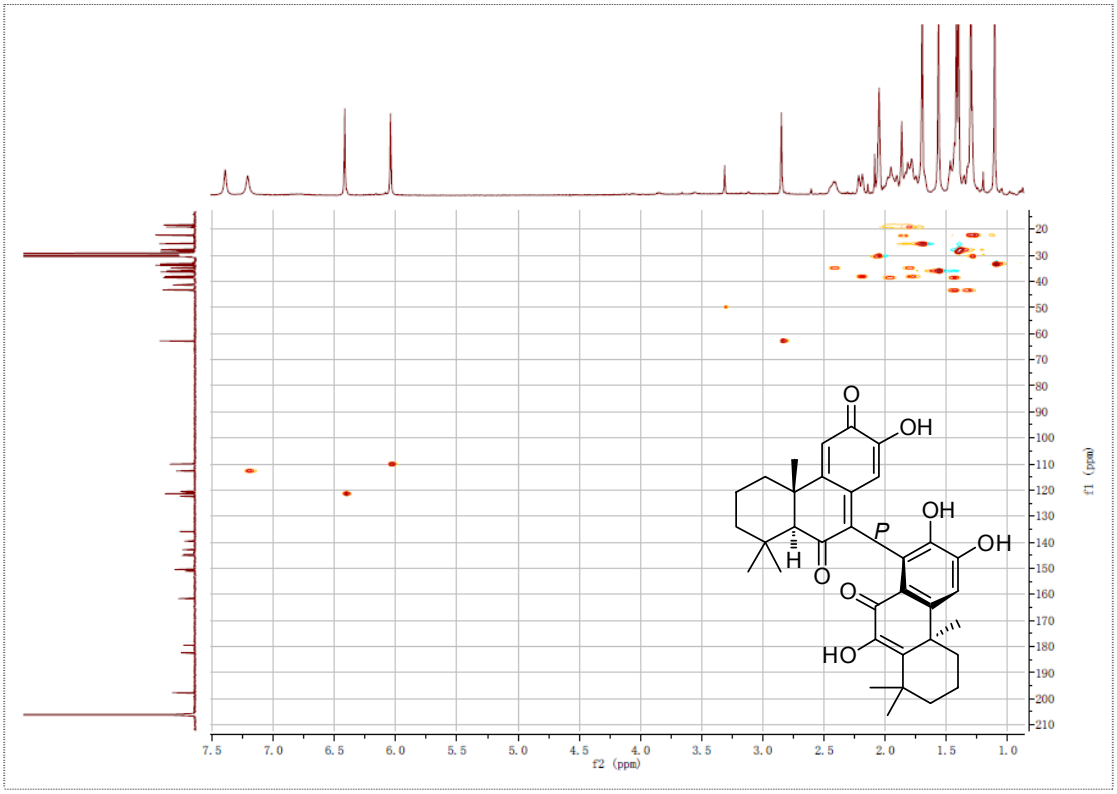

Figure S18. HSQC spectrum of (*P*)-bicelaphanol A (**2**) in acetone-d_6.

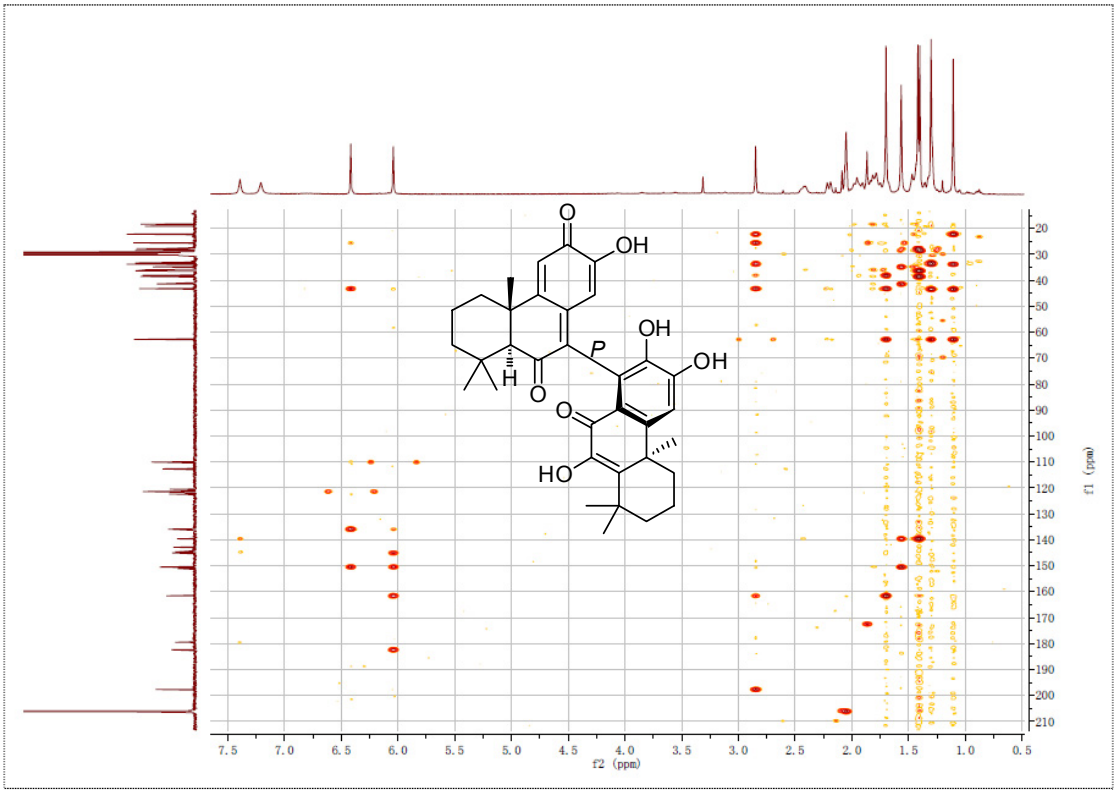

Figure S19. HMBC spectrum of (*P*)-bicelaphanol A (**2**) in acetone-d_6.

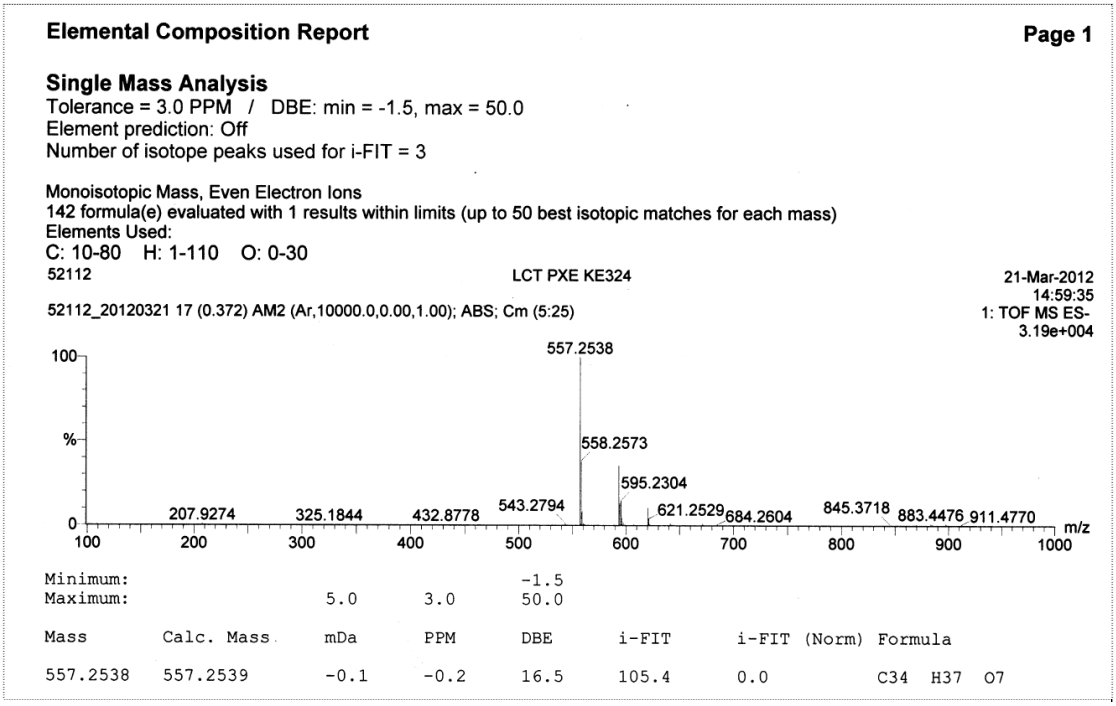

Figure S20. HRESI-MS spectrum of (*P*)-bicelaphanol A (**2**).

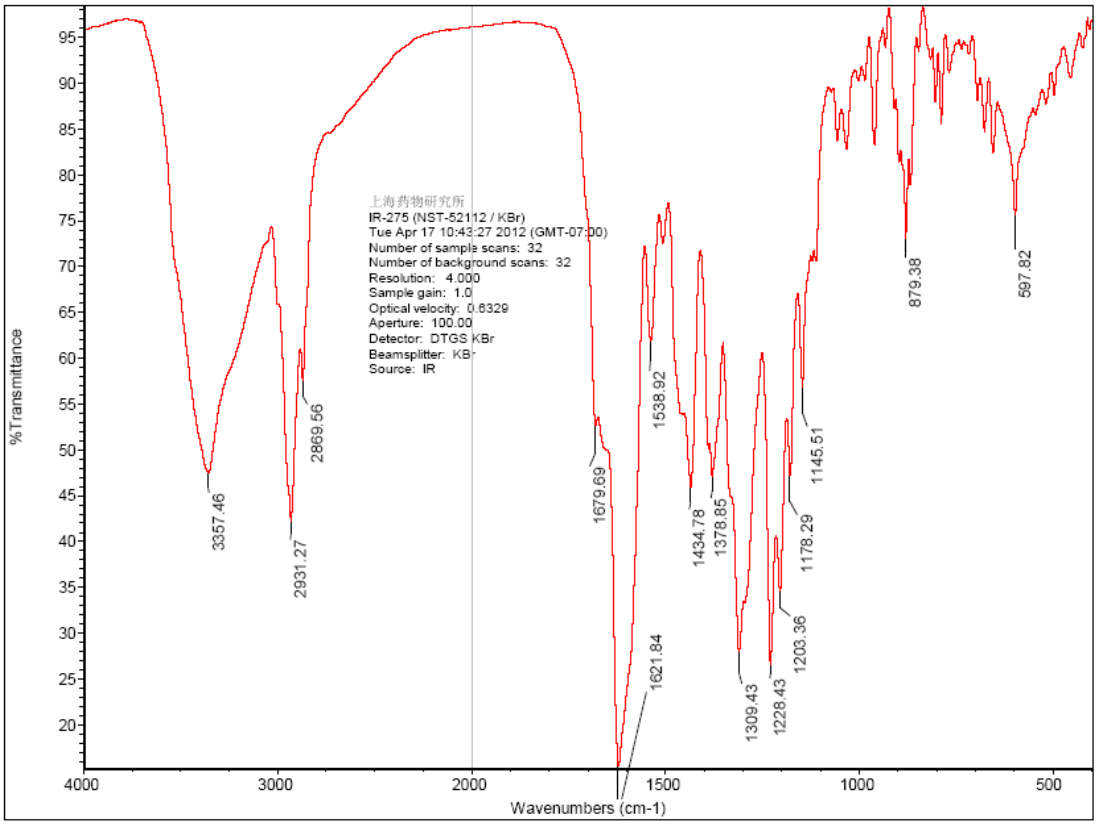

Figure S21. IR spectrum of (*P*)-bicelaphanol A (**2**).

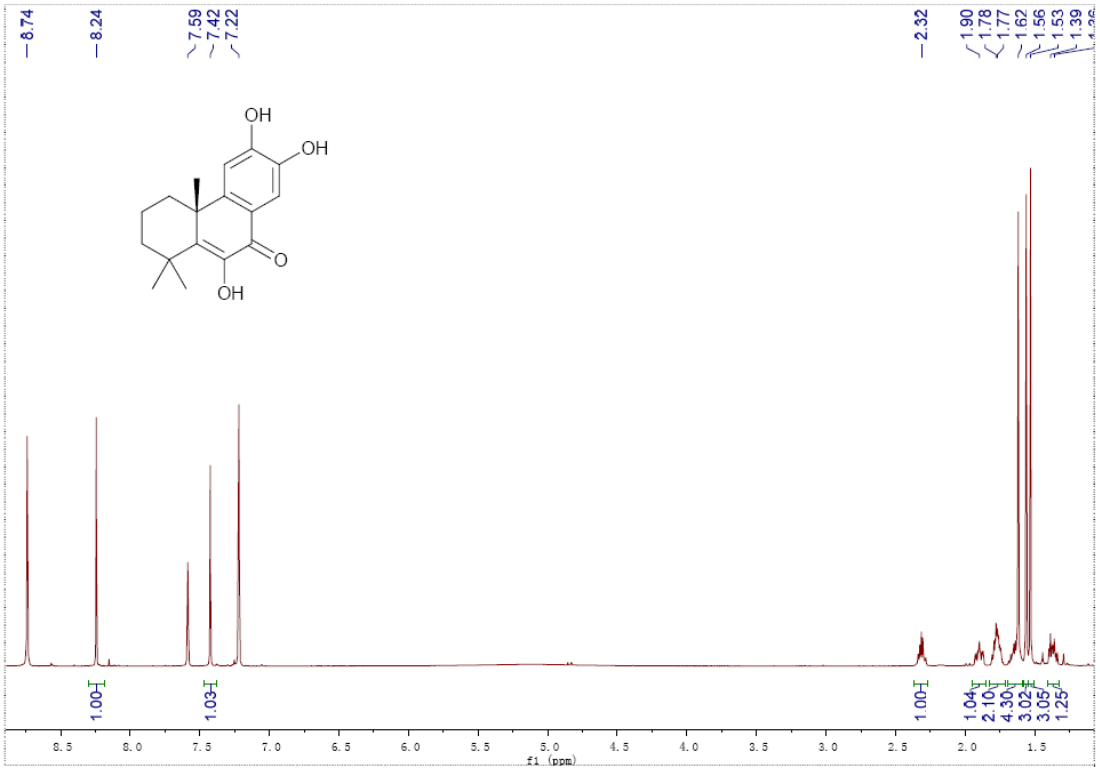

Figure S22. [1]H NMR spectrum of celaphanol A (**3**) in pyridine-d_5 (400 MHz).

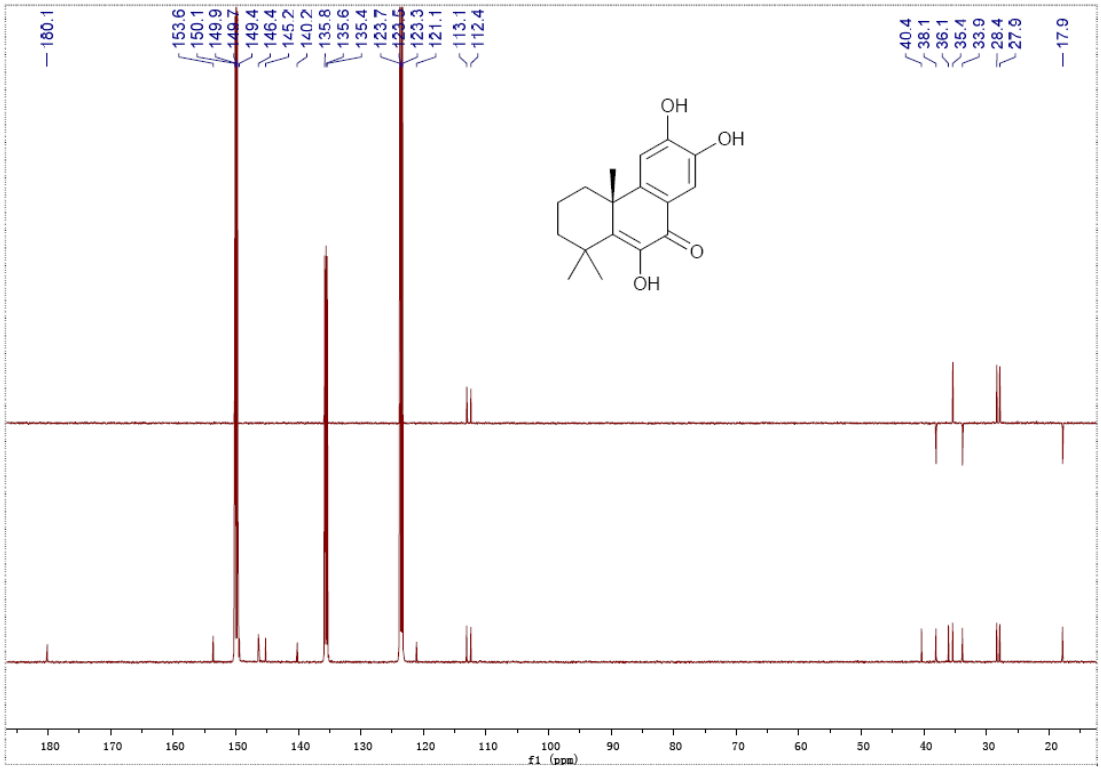

Figure S23. [13]C NMR spectrum of celaphanol A (**3**) in pyridine-d_5 (100 MHz).

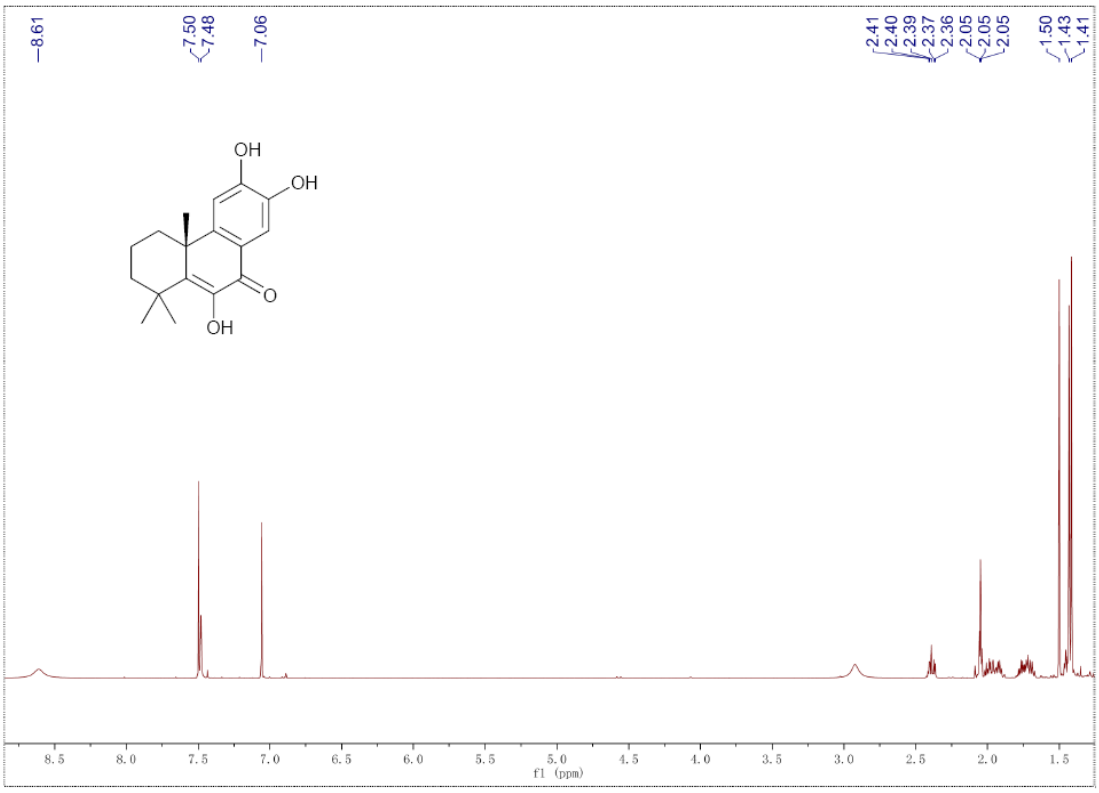

Figure S24. ^{1}H NMR spectrum of celaphanol A (**3**) in acetone-d_6 (400 MHz).

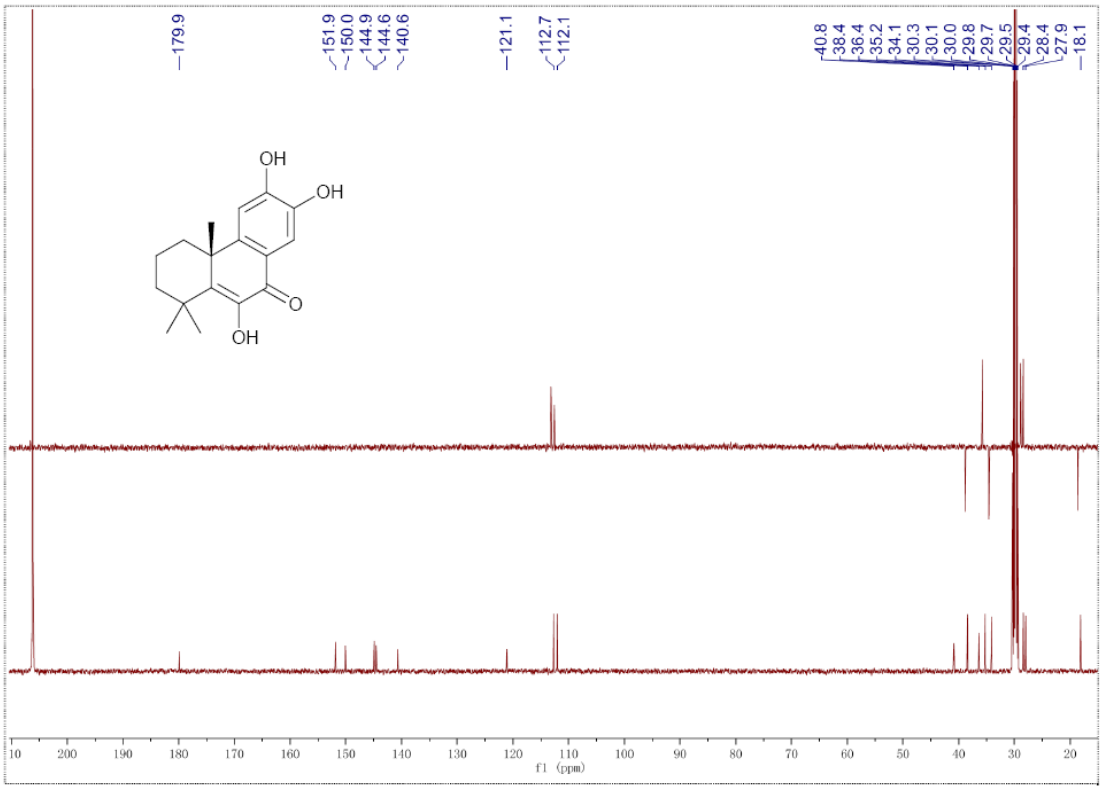

Figure S25. ^{13}C NMR spectrum of celaphanol A (**3**) in acetone-d_6 (100 MHz).

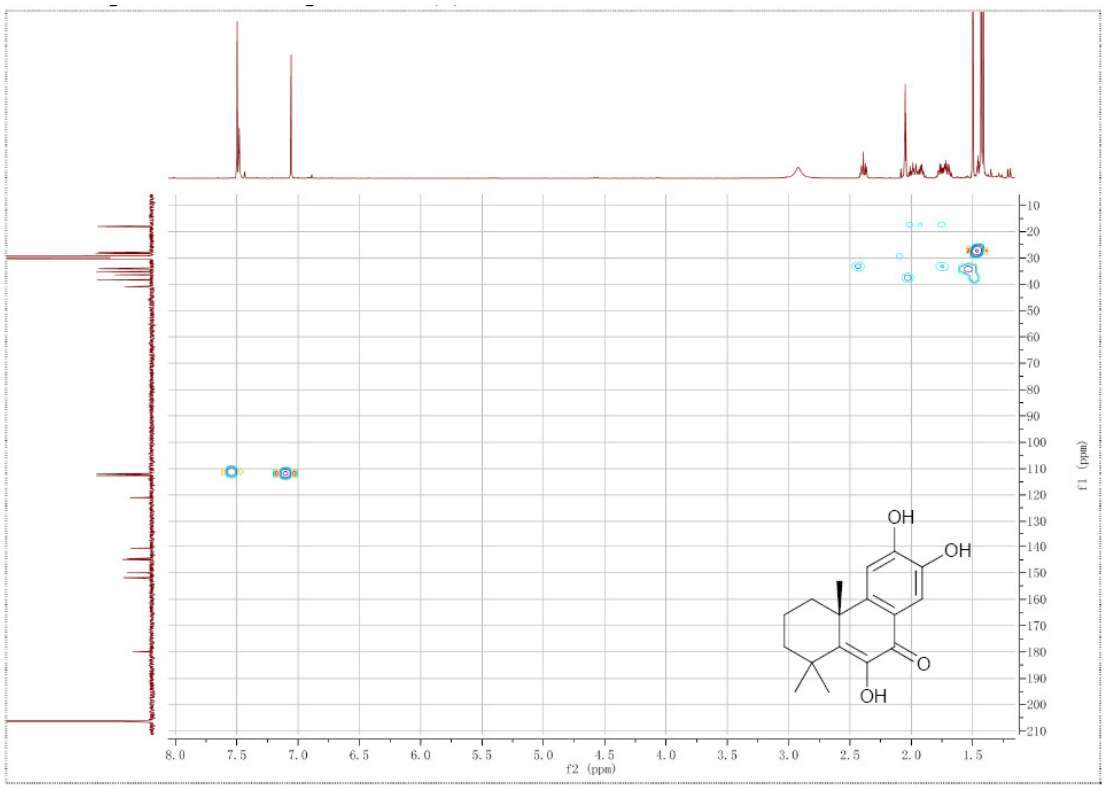

Figure S26. HSQC spectrum of celaphanol A (**3**) in acetone-d_6.

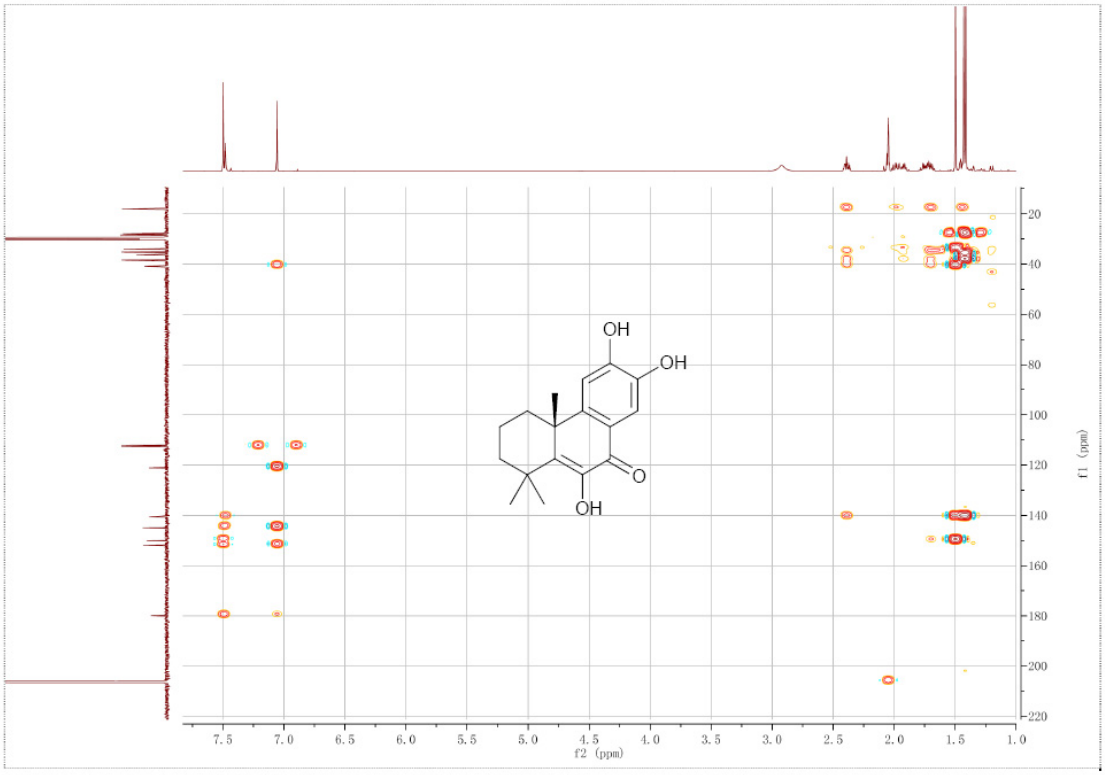

Figure S27. HMBC spectrum of celaphanol A (**3**) in acetone-d_6.

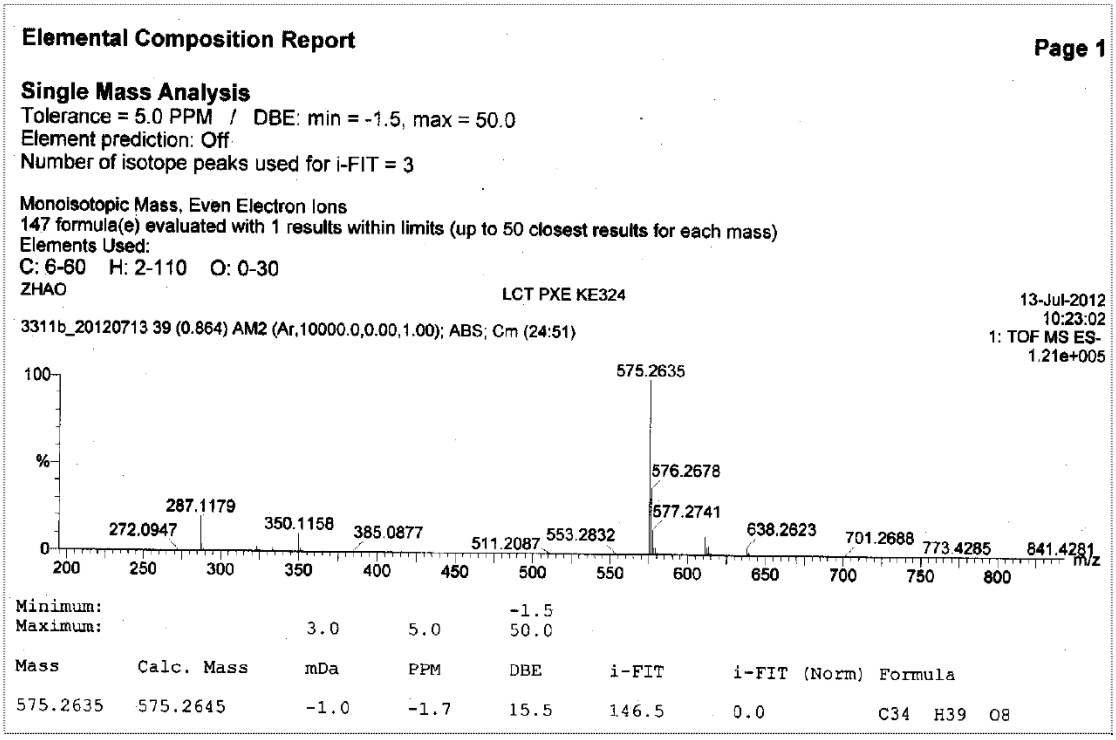

Figure S28 HRESI-MS spectrum of celaphanol A (**3**).